Journal of Structural Engineering & Applied Mechanics (2022) 5(3):143-160
DOI 10.31462/jseam.2022.03143160

RESEARCH ARTICLE

Advanced frequency analysis of thick FGM plates using third-order shear deformation theory with a nonlinear shear correction coefficient

C.C. Hong

Hsiuping University of Science and Technology, Department of Mechanical Engineering, Taichung, Taiwan

Article History

Received 06 June 2022
Accepted 21 August 2022

Keywords

Third-order shear deformation theory
FGM
Fully homogeneous equation
Vibration
Nonlinear

Abstract

The effects of third-order shear deformation theory (TSDT) displacements and advanced nonlinear varied shear correction coefficient on the free vibration frequency of thick functionally graded material (FGM) plates under environment temperature are studied. The nonlinear coefficient term of TSDT displacements is included to derive the advanced equation of nonlinear varied shear correction coefficient for the thick FGM plates. The determinant of the coefficient matrix in dynamic equilibrium differential equations under free vibration can be represented into fully homogeneous equation and the natural frequency can be found. The parametric effects of nonlinear coefficient term of TSDT, environment temperature and FGM power law index on the natural frequency of thick FGM plates are investigated.

1. Introduction

It is very interesting to introduce the method to obtain the frequency of free vibration for thick plates with length to thickness ratio less than 10. There are many ways used for the free vibration frequency, e.g. the hardware experiment, the computer by using commercial software and by using custom package. It would be more expensive by the experiment way of isolated sound room to obtain vibration frequency than by the computer software. The vibration frequency of the thick plates usually found to be the fundamental frequency and avoided to be in the resonance condition with the rotational machinery in the practical equipments. Some of the commercial software might used only the simply and basic eigenvalue equation for the determinant value of vibration frequency. It would be more importance to have the value of vibration frequency by considering the effects of nonlinear third-order of thickness z direction, e.g. z^3 in term of coefficient c_1 for third-order shear deformation theory (TSDT) of displacements. Also considering the advanced nonlinear varied value of shear correction coefficient used for the stiffness integration and the environment temperature used for the functionally graded material (FGM) plates.

There are numerous papers on the investigations of free vibration frequency for the plates. In 2020, Gunasekaran et al. [1] presented an analytical investigation on free vibration frequencies by using a TSDT of displacements for the graphene reinforced composite (GRC) FGM plate. The one directional angular frequency with time is used in the analysis of vibrations. In 2020, Vinyas [2] presented the frequency response by using a higher order shear deformation theory (HSDT) of displacements for the circular and

Correspondence C.C Hong cchong@mail.hust.edu.tw

annular porous magneto-electro-elastic (P-MEE) FGM plates. In 2019, Alaimo et al. [3] presented an analytical investigation on the damped free-vibration by using Galerkin method to approximate the fourth-order expansion of displacements for the composited viscoelastic plates. In 2019, Vinyas et al. [4] presented a coupled frequency response by using the TSDT of displacements for composited magneto-electro-elastic plates. In 2019, Karsh et al. [5] presented a low-frequency free vibration analysis by using first-order shear deformation theory (FSDT) of displacements for the FGM plates. In 2019, Gao et al. [6] presented a low frequency analysis by using the commercial package COMSOL for the cavities containing N-beam resonators in the metamaterial plates. In 2018, Geng et al. [7] presented the mid-frequency analysis by using B-spline wavelet on interval finite element method (FEM) for the thin plates. In 2018, Morozov and Lopatin [8] presented the fundamental frequency analysis by using the Galerkin method for the anisotropic laminated composite plates. In 2017, Lee et al. [9] presented the natural frequency analysis by using the homotopy perturbation method (HPM) for the thin plates in two directional angular frequency with time, e.g. two mode shapes in subscript numbers (m, n) of natural frequency. In 2017, Rezaei et al. [10] presented the free vibration analysis by using a simple FSDT of displacements for the porosities FGM plates. These frequency studies usually did not have two directions of mode vibrations in time, also not considering the shear correction coefficient effect of shear stresses, especially in the thick plates.

When the values of free vibration frequency were obtained, then they can be used as the initial value for the further appropriate studies in the thermal vibration and transient response. The first smaller values e.g. five values of free vibration frequency were used as the fundamental frequencies to study further, also it would be interesting to study further about more than one directional angular frequency with respective to length direction, width direction of plates and time. The author has some preliminary investigations of vibration frequencies for thick FGM shells without considering the effects of nonlinear coefficient term of TSDT displacements on the calculation of varied shear correction coefficient. In 2020, Hong [11] presented the preliminary calculation of free vibration frequencies by using the TSDT displacements for the thick FGM spherical shells with simply homogeneous equation. In 2020, Hong [12] presented the preliminary calculation of free vibration frequencies by using the TSDT displacements for the thick FGM circular cylindrical shells with simply homogeneous equation. There are also some thermal vibration investigations in the Terfenol-D FGM plates without considering the effects of nonlinear coefficient term of TSDT displacements on the calculation of varied shear correction coefficient. In 2014, Hong [13] presented the thermal vibration of Terfenol-D FGM plates by preliminary considering the effects of FSDT model and the varied modified shear correction factor to obtain the computational results. In 2012, Hong [14] presented the rapid heating for Terfenol-D FGM plates by preliminary considering the effect of FSDT model to obtain the computational results.

It is interesting to study further about the free vibration frequencies of thick FGM plates in simultaneously considering the effects of the TSDT of displacements, the nonlinear shear correction coefficient, environment temperature and the two directions of mode vibrations in time with fully homogeneous equation under four edges simply supported boundary conditions. The main motivations and issues for this paper are the advanced nonlinear shear correction coefficient kα for the thick FGM plates is used in the calculation of stiffness integration, also introduced the advanced nonlinear k_α topic for the computation of free vibration frequencies including the effect of coefficient c_1 term of TSDT, power-law exponent of FGM and environment temperature. It is an extension of some previous papers by the author. It is the novelty of the computation work in free vibration frequencies of thick FGM plates by using and considering the varied effect of advanced nonlinear k_α, e.g. the values of advanced kαare usually in nonlinear with coefficient c_1, power-law exponent of FGM and environment temperature.

2. Formulation procedures for the advanced nonlinear k_α

For the free vibration of a composited two-material thick FGM plate under environment temperature T is studied with thickness h_1 and h_2 of FGM constituent material 1 and FGM constituent material 2 respectively, length a, width b of the FGM plate are shown in Fig. 1. The properties P_i of individual constituent material of FGMs are functions of T and temperature coefficients P_0, P_{-1}, P_1, P_2, and P_3 [14]. The material properties of power-law function of FGM plates are considered with the dominated Young's modulus E_{fgm} of FGMs in standard variation form of power-law exponent parameter R_n, the others are assumed in the simple average form for the Poisson's ratio ν_{fgm}, density, thermal expansion coefficient, thermal conductivity and specific heat [15-16].

The time dependent of displacements u, v and w of thick FGM plates are assumed in the nonlinear coefficient c_1 term of TSDT equations [17] as follows:

$$\begin{aligned} u &= u^0(x,y,t) + z\psi_x(x,y,t) - c_1 z^3\left(\psi_x + \frac{\partial w}{\partial x}\right) \\ v &= v^0(x,y,t) + z\psi_y(x,y,t) - c_1 z^3\left(\psi_y + \frac{\partial w}{\partial y}\right) \\ w &= w(x,y,t) \end{aligned} \tag{1}$$

where u^0 and v^0 are displacements in the direction of x and y axes, respectively, w is transverse displacement in the direction of z axis of the middle-plane of thick FGM plates. ψ_x and ψ_y are the shear rotations. t is the time. The coefficient for $c_1 = 4/(3h^{*2})$ is given as in TSDT approach, in which h^* is the total thickness of thick FGM plates. x, y and z are the coordinates in the Cartesian axes system.

By defining the following expressions integrated with the stiffness $\bar{Q}_{i^s j^s}$ and $\bar{Q}_{i^* j^*}$ in the direction of z axis for the thick FGM plates

$$\begin{aligned} (A_{i^s j^s}, B_{i^s j^s}, D_{i^s j^s}, E_{i^s j^s}, F_{i^s j^s}, H_{i^s j^s}) &= \int_{-h^*/2}^{h^*/2} \bar{Q}_{i^s j^s}(1, z, z^2, z^3, z^4, z^6)\,dz\,, \quad (i^s, j^s = 1,2,6) \\ (A_{i^* j^*}, B_{i^* j^*}, D_{i^* j^*}, E_{i^* j^*}, F_{i^* j^*}, H_{i^* j^*}) &= \int_{-h^*/2}^{h^*/2} k_\alpha \bar{Q}_{i^* j^*}(1, z, z^2, z^3, z^4, z^5)\,dz\,, \quad (i^*, j^* = 4,5) \end{aligned} \tag{2}$$

with total number of constituent layers $N^* = 2$ and $\rho^{(k)}$ is the density of superscript k^{th} constituent ply. k_α is the shear correction coefficient in advanced nonlinear varied value. The stiffness $\bar{Q}_{i^s j^s}$ and $\bar{Q}_{i^* j^*}$ for thick FGM plates can be used in simple forms as follows by Shen [18]:

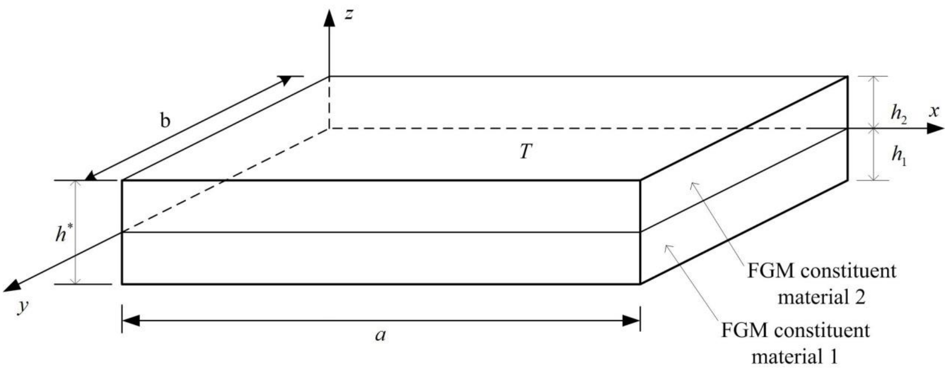

Fig. 1. Composited two-material thick FGM plate

$$\bar{Q}_{11} = \bar{Q}_{22} = \frac{E_{fgm}}{1-\nu_{fgm}{}^2}$$
$$\bar{Q}_{12} = \frac{\nu_{fgm} E_{fgm}}{1-\nu_{fgm}{}^2}$$
$$\bar{Q}_{44} = \bar{Q}_{55} = \bar{Q}_{66} = \frac{E_{fgm}}{2(1+\nu_{fgm})} \tag{3}$$
$$\bar{Q}_{16} = \bar{Q}_{26} = \bar{Q}_{45} = 0$$

in which $E_{fgm} = (E_2 - E_1)[(z + h^*/2)/h^*]^{Rn} + E_1$ and $v_{fgm} = (v_1 + v_2)/2$. E_1 and E_2 are the Young's modulus. v_1 and v_2 are the Poisson's ratios of the FGM constituent material 1 and 2, respectively.

When the varied shear correction coefficient is considered the effects simultaneously from coefficient c_1 term of TSDT, power-law exponent of FGM and environment temperature, thus, the advanced nonlinear varied shear correction coefficient might be called in the preliminary study. The advanced nonlinear k_α can be obtained as follows for the thick FGM plates by using the equivalence principle of total strain energy. The more detail for the derivation of the k_α is based on the determination in 2014 by Hong [13], but the current expression including with c_1 term after advanced derivation and without magnetostrictive term.

$$k_\alpha = \frac{1}{h^*} \frac{FGMZSV}{FGMZIV} \tag{4}$$

where $FGMZSV = (FGMZS - c_1 FGMZSN)^2$ is in function of h^{*6}, $FGMZIV = FGMZI - 2c_1 FGMZIV1 + c_1^2 FGMZIV2$ is in function of h^{*5} , in which $FGMZS$, $FGMZSN$, $FGMZI$, $FGMZIV1$ and $FGMZIV2$ parameters can be expressed in functions of E_1, E_2, h^* and R_n for the thick FGM plates. The values of advanced nonlinear k_α are usually functions of c_1, R_n and T, but independent to the values of h^*.

The vibration frequency (ω_{mn} with two directional mode shape subscript numbers m and n) for four sides simply supported boundary condition with not symmetrical ($B_{ij} \neq 0$, $I_1 \neq 0$, $I_3 \neq 0$, $J_1 \neq 0$) thick FGM plates can be derived by assuming that $A_{16} = A_{26} = 0$, $D_{16} = D_{26} = 0$, $E_{16} = E_{26} = 0$, $F_{16} = F_{26} = 0$, $H_{16} = H_{26} = 0$ and $A_{45} = D_{45} = F_{45} = 0$ under the following sinusoidal displacement forms with amplitudes a_{mn}, b_{mn}, c_{mn}, d_{mn} and e_{mn}.

$$\begin{aligned} u^0 &= a_{mn} \cos(m\pi x/a)\sin(n\pi y/b)\sin(\omega_{mn} t) \\ v^0 &= b_{mn} \sin(m\pi x/a)\cos(n\pi y/b)\sin(\omega_{mn} t) \\ w &= c_{mn} \sin(m\pi x/a)\sin(n\pi y/b)\sin(\omega_{mn} t) \\ \psi_x &= d_{mn} \cos(m\pi x/a)\sin(n\pi y/b)\sin(\omega_{mn} t) \\ \psi_y &= e_{mn} \sin(m\pi x/a)\cos(n\pi y/b)\sin(\omega_{mn} t) \end{aligned} \tag{5}$$

By substituting equations (5) into dynamic equilibrium differential equations (A1) with TSDT of thick FGM plates under T in terms of partial derivatives of displacements and shear rotations under free vibration (without the thermal loads and mechanical loads), thus the fully homogeneous equation (A2) can be obtained and the ω_{mn} can be found. More detailed procedures were presented in Hong [19]. The dynamic equilibrium differential equations and the fully homogeneous equation are listed in the Appendix.

3. Some numerical results and discussions

The composite FGM SUS304/Si_3N_4 material is used to implement the numerical computation under T (free stress assumed). The FGM constituent material 1 at lower position is SUS304, the FGM constituent material 2 at upper position is Si_3N_4 used for the free vibration frequency computations.

Firstly, the calculated values of advanced nonlinear k_α are shown in Table 1. By considering the effect of c_1 on k_α for a/b = 1 and $h_1 = h_2$, the advanced computational values of k_α under T = 1 K are presented. For the value c_1 = 92.592598/mm^2 decreases to c_1= 0.0092592/mm^2, the $k_\alpha$values are increasing firstly then decreasing with R_n. For the value c_1 = 0/mm^2, the k_α values are also increasing firstly then decreasing with R_n. The advanced k_α values are found in functions of c_1, R_n and T, but independent to the values of h^* for the thick FGM plates.

Fig. 2. shows that varied values of k_α vs. T under R_n = 0.5, 1 and 10 for the values $c_1 \neq 0$ and $c_1 = 0$ cases, respectively. The k_α values in $c_1 \neq 0$ case are smaller than that in $c_1 = 0$ case. The k_α values are nearly close to 1.3 for R_n = 0.5 and 1, also are nearly close to 1.1 for R_n = 10 in $c_1 = 0$ case. The k_α values found in the c_1 = 0 case can be considered in overestimated values for the thick FGM plates.

Thus, advanced computational values of k_α for $c_1 \neq 0$ case are used in frequency calculations of the free vibration ($\Delta T = 0$). For the dimensionless frequency parameter defined as $f^* = \omega_{11} h^* (\rho_2/E_2)^{0.5}$ and value is shown in Table 2, where ω_{11} is the fundamental first natural frequency (subscript $m = n = 1$), ρ_2 is the density of FGM constituent material 2. With h^*= 1.2 mm, the f^*values are not greater than 0.001379 under T = 1 K, 100 K, 300 K, 600 K and 1000 K. f^*= 0.001379 is the maximum value that occurs at a/h^*= 8, R_n = 2 and T = 600 K for the thick FGM plates.

Table 1. Nonlinear varied k_α vs. c_1 and R_n under T = 1 K

c_1 (1/mm^2)	h^* (mm)	k_α						
		R_n = 0.1	R_n = 0.2	R_n = 0.5	R_n = 1	R_n = 2	R_n = 5	R_n = 10
92.592598	0.12	-0.323869	-0.324963	-0.365392	-0.541369	-2.399161	0.802957	0.518229
0.925925	1.2	-0.323870	-0.324963	-0.365392	-0.541370	-2.399165	0.802958	0.518229
0.231481	2.4	-0.323869	-0.324963	-0.365392	-0.541370	-2.399165	0.802958	0.518229
0.037037	6	-0.323869	-0.324962	-0.365392	-0.541370	-2.399163	0.802957	0.518229
0.009259	12	-0.323870	-0.324962	-0.365392	-0.541370	-2.399163	0.802957	0.518229
0	0.12	0.915601	0.992033	1.175883	1.340146	1.396886	1.249938	1.099855
0	1.2	0.915601	0.992030	1.175884	1.340146	1.396886	1.249938	1.099855
0	2.4	0.915601	0.992030	1.175884	1.340146	1.396886	1.249938	1.099855
0	6	0.915600	0.992028	1.175884	1.340146	1.396886	1.249938	1.099855
0	12	0.915600	0.992027	1.175884	1.340146	1.396886	1.249938	1.099855

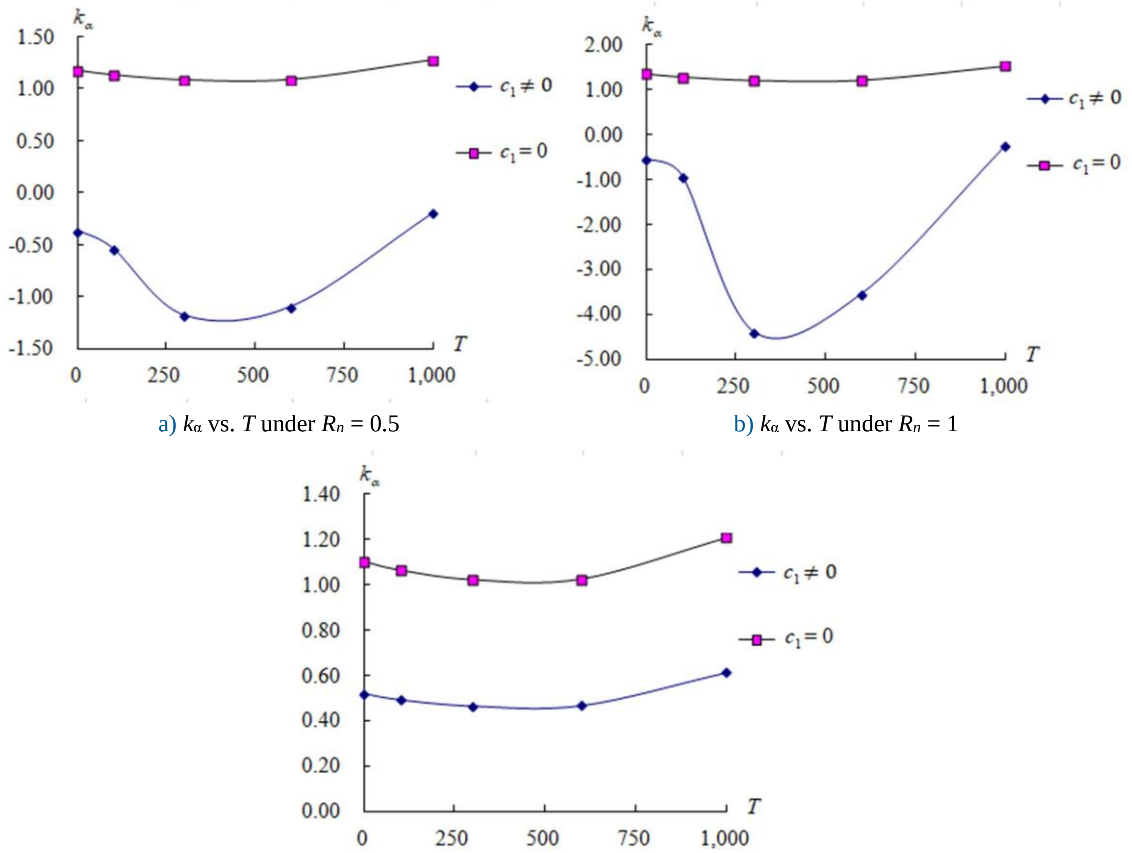

a) k_α vs. T under R_n = 0.5

b) k_α vs. T under R_n = 1

c) k_α vs. T under R_n = 10

Fig. 2. k_α vs. T under R_n = 0.5, 1 and 10 for the values $c_1 \neq 0$ and $c_1 = 0$

Table 2. f^* for SUS304/Si_3N_4

a/h^*	R_n	Present solution f^* (h^*= 1.2 mm, $c_1 = 4/(3h^{*2})$, nonlinearly varied k_α)				
		T = 1 K	T = 100 K	T = 300 K	T = 600 K	T = 1000 K
5	0.5	0.000117	0.000114	0.000100	0.000111	0.000166
	1	0.000111	0.000103	0.000063	0.000075	0.000164
	2	0.000077	0.000133	0.000488	0.000502	0.000154
	10	0.000304	0.000313	0.000333	0.000363	0.000431
8	0.5	0.000158	0.000155	0.000137	0.000152	0.000223
	1	0.000151	0.000140	0.000087	0.000103	0.000220
	2	0.000105	0.000206	0.001282	0.001379	0.000209
	10	0.000413	0.000427	0.000458	0.000500	0.000588
10	0.5	0.000194	0.000190	0.000168	0.000187	0.000275
	1	0.000185	0.000172	0.000106	0.000127	0.000272
	2	0.000129	0.000372	0.000318	0.000325	0.000258
	10	0.000540	0.000561	0.000610	0.000680	0.000887

The dimensionless frequency parameter defined as $\omega^*= (\omega_{11}b^2/\pi^2)(I_s/D_s)^{0.5}$ and value is shown in Table 3, where $I_s = \int_{-\frac{h^*}{2}}^{\frac{h^*}{2}} \rho_1 dz$, $D_s = \int_{-\frac{h^*}{2}}^{\frac{h^*}{2}} \bar{Q}_1 z^2 dz$, ρ_1 is the density of FGM constituent material 1, $\bar{Q}_1 = E_1/(1 - \nu_1^2)$ of FGM constituent material 1. With $h^*= 1.2$ mm, the ω^* values are not greater than 0.075554 under T = 1 K, 100 K, 300 K, 600 K and 1000 K. $\omega^*= 0.075554$ is the maximum value that occurs at $a/h^*=10$, $R_n= 10$ and T = 1000 K for the thick FGM plates.

The dimensionless frequency parameter defined as $\Omega = (\omega_{11}a^2/h^*)[\rho_1(1-\nu_1^2)/E_1]^{0.5}$ and value is shown in Table 4. With $h^*= 1.2$ mm, the Ω values are not greater than 0.215261 under T = 1 K, 100 K, 300 K, 600 K and 1000 K. $\Omega = 0.215261$ is the maximum value that occurs at $a/h^*= 10$, $R_n = 10$ and T = 1000 K for the thick FGM plates.

It is interesting to compare the present solution of free vibration values of dimensionless frequency for $c_1 \neq 0$ case with some authors' work as shown in the Table 5-7. The values of f^* vs. h^* for SUS304/Si_3N_4 under $a/h^*= 10$ and T = 300 K with advanced k_α effect are shown in Table 5. The value $f^*= 0.084531$ at $h^*=$ 14 mm and $R_n = 2$ is found in close to $f^*= 0.0839$ for Al/ZrO_2 under no environmental temperature effect in Jha et al. [20].

The values of ω^* vs. h^* for SUS304/Si_3N_4 under $a/h^*= 10$ and T = 300 K with advanced k_α effect are shown in Table 6. The value $\omega^*= 3.879621$ at $h^*= 10$ mm, $R_n = 2$ is found in close to $\omega^*= 4.1165$ for $h^*= 200$ mm forced vibration under uniform temperature rise ($\Delta T= 0$) by Kim [21]. Also compare the value $\omega^*=$ 3.879621 is in close with $\omega^*= 3.99244$ for uniform distribution (UD) in CNTRC FGM plates resting on Winkler–Pasternak elastic foundations by Duc et al. [22].

Table 3. ω^* for SUS304/Si_3N_4

a/h^*	R_n	Present solution ω^* ($h^*= 1.2$ mm, $c_1 = 4/(3h^{*2})$, nonlinearly varied k_α)				
		T = 1 K	T = 100 K	T = 300 K	T = 600 K	T = 1000 K
5	0.5	0.002388	0.002260	0.001917	0.002124	0.003552
	1	0.002266	0.002034	0.001211	0.001436	0.003498
	2	0.001566	0.002622	0.009293	0.009540	0.003290
	10	0.006171	0.006175	0.006356	0.006893	0.009188
8	0.5	0.008239	0.007836	0.006696	0.007417	0.012165
	1	0.007853	0.007087	0.004258	0.005046	0.012030
	2	0.005490	0.010437	0.062493	0.067049	0.011413
	10	0.021440	0.021569	0.022366	0.024343	0.032050
10	0.5	0.015773	0.015011	0.012826	0.014223	0.023413
	1	0.015037	0.013571	0.008136	0.009652	0.023164
	2	0.010498	0.029382	0.024273	0.024685	0.021992
	10	0.043841	0.044310	0.046484	0.051713	0.075554

Table 4. Ω for $SUS304/Si_3N_4$

a/h^*	R_n	Present solution Ω (h^*= 1.2 mm, $c_1 = 4/(3h^{*2})$, nonlinearly varied k_α)				
		T = 1 K	T = 100 K	T = 300 K	T = 600 K	T = 1000 K
5	0.5	0.006805	0.006441	0.005463	0.006052	0.010122
	1	0.006457	0.005796	0.003452	0.004094	0.009966
	2	0.004464	0.007472	0.026478	0.027183	0.009376
	10	0.017583	0.017595	0.018111	0.019639	0.026177
8	0.5	0.023474	0.022326	0.019078	0.021132	0.034659
	1	0.022376	0.020192	0.012131	0.014379	0.034275
	2	0.015641	0.029737	0.178050	0.191030	0.032518
	10	0.061085	0.061455	0.063724	0.069357	0.091315
10	0.5	0.044941	0.042770	0.036543	0.040525	0.066708
	1	0.042842	0.038665	0.023182	0.027499	0.065999
	2	0.029910	0.083713	0.069157	0.070331	0.062659
	10	0.124910	0.126245	0.132438	0.147336	0.215261

Table 5. Comparison of frequency f^* for $SUS304/Si_3N_4$ and Al/ZrO_2

c_1 (1/mm^2)	h^* (mm)	f			
		Present solution, a/h^*= 10, T = 300 K, nonlinearly varied k_α for $SUS304/Si_3N_4$			Jha et al. [20] Al/ZrO_2, R_n = 0.5
		R_n = 0.5	R_n = 1	R_n = 2	
0.925925	1.2	0.000168	0.000106	0.000318	--
0.333333	2	0.003663	0.003747	0.003847	--
0.013333	10	0.047598	0.049180	0.050952	--
0.009259	12	0.062619	0.064708	0.067043	--
0.006802	14	0.078943	0.081585	0.084531	0.0839

Table 6.Comparison of frequency ω^* for $SUS304/Si_3N_4$

c_1 (1/mm^2)	h^* (mm)	ω^*				
		Present solution, a/h^*= 10, T = 300 K, nonlinearly varied k_α			Kim 2005 [21] Forced vibration, h^*=200 mm, ΔT = 0	Duc et al. [22] CNTRC, FSDT
		R_n= 0.5	R_n= 1	R_n= 2	R_n= 2	UD type
0.925925	1.2	0.012826	0.008136	0.024273	--	--
0.333333	2	0.278953	0.285340	0.292981	--	--
0.013333	10	3.624274	3.744695	3.879621	4.1165	3.99244
0.009259	12	4.767975	4.927086	5.104831	--	--
0.006802	14	6.010954	6.212089	6.436427	--	--

Table 7. Comparison of frequency Ω for $SUS304/Si_3N_4$

c_1 (1/mm^2)	h^* (mm)	Ω: Present solution, a/h^*= 10, T= 300 K, nonlinear varied k_α			Ungbhakorn and Wattanasakulpong [23], ΔT = 400 K, R_n = 1
		R_n = 0.5	R_n = 1	R_n = 2	
0.925925	1.2	0.036543	0.023182	0.069157	--
0.333333	2	0.794768	0.812965	0.834735	--
0.053333	5	3.613396	3.728638	3.862379	--
0.037037	6	4.772100	4.926843	5.103842	5.359
0.013333	10	10.325957	10.669049	11.053467	--

The values of Ω vs. $h^*$for $SUS304/Si_3N_4$ under a/h^* = 10 and T = 300 K with advanced k_α effect are shown in Table 7. The value Ω = 5.103842 at h^*= 6 mm, R_n = 2 is found in close to Ω = 5.359 for forced vibration under temperature rise (ΔT = 400 K) by Ungbhakorn and Wattanasakulpong [23]. The values of dimensionless natural frequency parameters are also found in functions of a/h^*, R_n, c_1 and T for the thick FGM plates. Since the comparisons listed in Tables 5-7 are currently referred from the web site, it can be considered as a preliminary reference data, it might need to be provided in more precise results in the future studies.

Secondly, the natural frequency ω_{mn} values (unit 1/s) of free vibration are calculated according to mode shape numbers m and n for the thick $SUS304/Si_3N_4$ FGM plate with advanced k_α effect. The values of fundamental first (subscript m = n = 1) natural frequency ω_{11} vs. R_n are shown in Table 8 with c_1 = 0.925925/mm^2 under T = 1 K, 100 K, 300 K, 600 K and 1000 K. The results of fundamental first natural frequencies are found in functions of a/h^*, R_n, c_1 and T .

The values of natural frequency ω_{mn} vs. subscripts m, n = 1,2,...,9 are shown in Table 9 with R_n = 0.5, T = 300 K and c_1 = 0.925925/mm^2. The results of dimensional natural frequencies are found in varied with mode values m, n and a/h^* for the thick FGM plates.

Fig. 3 shows the values of ω_{1n} vs. R_n with c_1 = 0.925925/mm^2 and advanced k_α effect for thick FGM plate a/h^*= 5 and 10, respectively under T = 300 K. Generally the values of ω_{1n} are oscillating and going to around 0.005258 at n = 9 for a/h^*= 5 and R_n = 10. The greatest value of ω_{16} = 0.033687 (unit 1/s) is found, then decreasing to value ω_{19} = 0.005258 (unit 1/s) for a/h^*= 5 and R_n = 10. The values of ω_{1n} are also oscillating and going to around 0.008937 at n = 9 for a/h^*= 10 and R_n = 10. The greatest value of ω_{17} = 0.016076 (unit 1/s) is found, then decreasing to value ω_{19} = 0.008937 (unit 1/s) for a/h^*= 10 and R_n = 10.

Fig. 4 shows the values of ω_{1n} vs. T with c_1 = 0.925925/mm^2 and advanced k_α effect for thick FGM plate a/h^*= 5 and 10, respectively under R_n = 0.5. Generally the values of ω_{1n} are oscillating and going to around 0.004688 at n = 9 for a/h^*= 5 and T = 600 K. The greatest value of ω_{14} = 0.043468 (unit 1/s) is found, then decreasing to value ω_{19} = 0.00809 (unit 1/s) for a/h^*= 5 and T = 1000 K. The greatest value of ω_{19} = 0.006839 (unit 1/s) is found, the smallest value of ω_{11} = 0.002744 is found for a/h^*= 10 and T = 300 K.

Finally, the compared ω_{1n} values vs. two approach types of fully homogeneous equation (A2) and simply homogeneous equation (A3) are also shows in Fig. 5 for R_n = 0.5, T = 300 K and a/h^*= 10.

Table 8. Fundamental natural frequency ω_{11} for nonlinear varied k_α, c_1, h^*= 1.2 mm

a/h^*	R_n	ω_{11}				
		T = 1 K	T = 100 K	T = 300 K	T = 600 K	T = 1000 K
5	0.5	0.002017	0.001928	0.001641	0.001751	0.002485
	1	0.001914	0.001735	0.001037	0.001184	0.002447
	2	0.001323	0.002237	0.007954	0.007866	0.002302
	10	0.005212	0.005268	0.005441	0.005683	0.006428
10	0.5	0.003330	0.003201	0.002744	0.002932	0.004095
	1	0.003175	0.002894	0.001741	0.001989	0.004052
	2	0.002216	0.006266	0.005194	0.005088	0.003847
	10	0.009257	0.009449	0.009946	0.010659	0.013216

Table 9. ω_{mn} vs. m and n under nonlinear varied k_α, c_1, R_n = 0.5 and T = 300 K

a/h^*	ω_{1n}								
	n = 1	n = 2	n = 3	n = 4	n = 5	n = 6	n = 7	n = 8	n = 9
5	0.001641	0.001736	0.001821	0.001888	0.004822	0.029442	0.025729	0.021949	0.001641
10	0.002744	0.003067	0.003344	0.003466	0.003444	0.003340	0.003198	0.003038	0.006839
a/h^*	ω_{2n}								
	n = 1	n = 2	n = 3	n = 4	n = 5	n = 6	n = 7	n = 8	n = 9
5	0.001228	0.001264	0.001310	0.001375	0.004485	0.023202	0.020780	0.006867	0.001228
10	0.001594	0.001641	0.001689	0.001736	0.001781	0.001821	0.001857	0.001888	0.007277
a/h^*	ω_{3n}								
	n = 1	n = 2	n = 3	n = 4	n = 5	n = 6	n = 7	n = 8	n = 9
5	0.001227	0.001258	0.001306	0.001386	0.004120	0.020777	0.007638	0.006320	0.005388
10	0.001315	0.001336	0.001359	0.001385	0.001412	0.001440	0.001471	0.001506	0.007551
a/h^*	ω_{4n}								
	n = 1	n = 2	n = 3	n = 4	n = 5	n = 6	n = 7	n = 8	n = 9
5	0.001429	0.001469	0.001541	0.001685	0.003293	0.007149	0.006383	0.005687	0.005073
10	0.001215	0.001228	0.001245	0.001264	0.001285	0.001310	0.001339	0.001375	0.007629
a/h^*	ω_{5n}								
	n = 1	n = 2	n = 3	n = 4	n = 5	n = 6	n = 7	n = 8	n = 9
5	0.002244	0.002307	0.002450	0.002876	0.003748	0.005017	0.011626	0.007413	0.006639
10	0.001192	0.001203	0.001217	0.001233	0.001254	0.001278	0.001309	0.001347	0.007546
a/h^*	ω_{6n}								
	n = 1	n = 2	n = 3	n = 4	n = 5	n = 6	n = 7	n = 8	n = 9
5	0.002169	0.001921	0.001724	0.004902	0.004421	0.004559	0.004830	0.004944	0.004891
10	0.001217	0.001227	0.001240	0.001258	0.001279	0.001306	0.001340	0.001386	0.007358

Table 9. Continued.

a/h^*	ω_{7n} $n = 1$	$n = 2$	$n = 3$	$n = 4$	$n = 5$	$n = 6$	$n = 7$	$n = 8$	$n = 9$
5	0.001213	0.001175	0.001126	0.004870	0.003826	0.003424	0.003294	0.003325	0.003431
10	0.001287	0.001297	0.001312	0.001331	0.001355	0.001387	0.001429	0.001489	0.007138

a/h^*	ω_{8n} $n = 1$	$n = 2$	$n = 3$	$n = 4$	$n = 5$	$n = 6$	$n = 7$	$n = 8$	$n = 9$
5	0.000898	0.000884	0.006903	0.004393	0.003469	0.003008	0.002761	0.002641	0.002612
10	0.001416	0.001429	0.001446	0.001469	0.001500	0.001541	0.001599	0.001685	0.007001

a/h^*	ω_{9n} $n = 1$	$n = 2$	$n = 3$	$n = 4$	$n = 5$	$n = 6$	$n = 7$	$n = 8$	$n = 9$
5	0.000730	0.014808	0.005387	0.003932	0.003189	0.002757	0.002489	0.002323	0.002228
10	0.001659	0.001674	0.001696	0.001727	0.001770	0.001830	0.001920	0.002068	0.007491

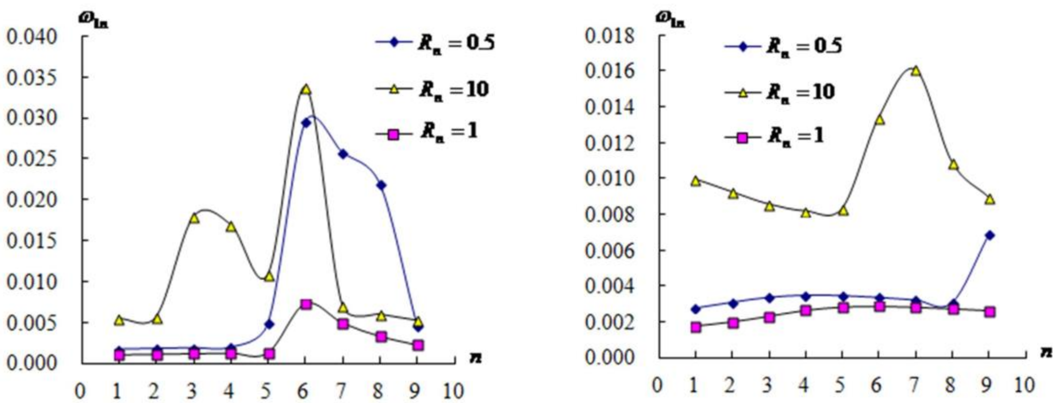

a) ω_{1n} vs. R_n for a/h^*= 5 b) ω_{1n} vs. R_n for a/h^*=10

Fig. 3. ω_{1n} vs. R_n for a/h^*= 5 and 10

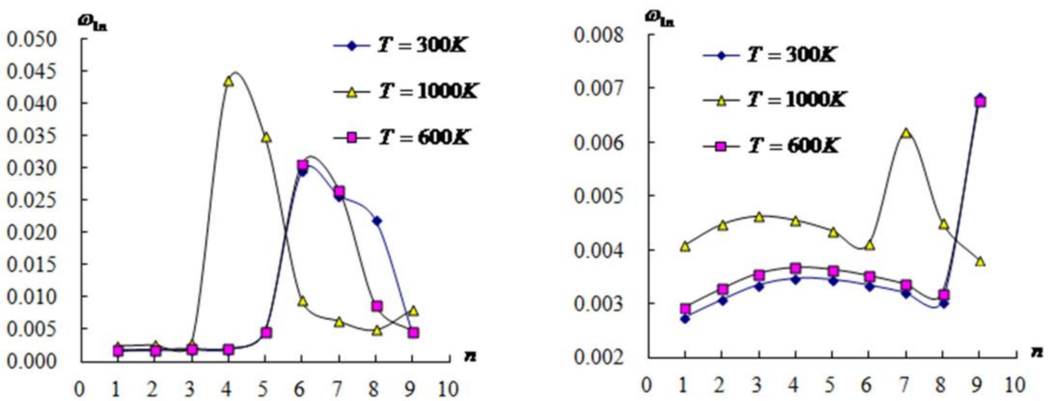

a) ω_{1n} vs. T for a/h^*= 5 b) ω_{1n} vs. T for a/h^*= 10

Fig. 4. ω_{1n} vs. T for a/h^*= 5 and 10

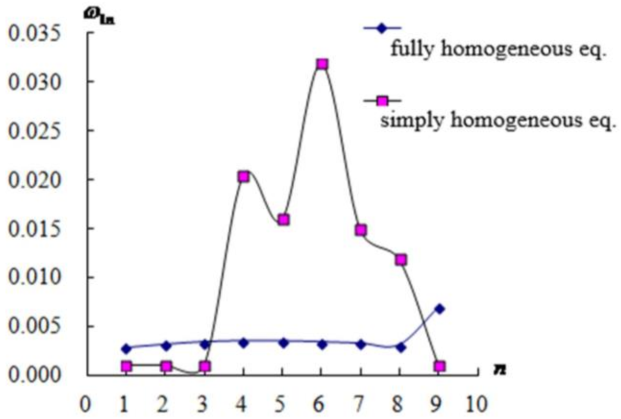

Fig. 5. Compared ω_{1n} vs. homogeneous equation for R_n= 0.5, T= 300K and a/h^*= 10

The ω_{1n} values can be considered in overestimated for simply homogeneous equation with respect to the values for fully homogeneous equation. For more detailed procedures about simply homogeneous equation, refer Hong [24]. The simply homogeneous equation is be listed in the Appendix.

4. Conclusions

The values of natural frequency ω_{mn} and three types of dimensionless frequency parameters are calculated with fully homogeneous equation in the free vibration of thick FGM plates by considering the effects of TSDT c_1 term, advanced nonlinear varied $k_\alpha$and environment temperature T. The advanced $k_\alpha$values are found in functions of c_1, R_n and T, but independent to the values of h^* for the thick FGM plates. The $k_\alpha$values found in the c_1 = 0 case can be considered in overestimated values for the thick FGM plates. The values of dimensionless natural frequency parameters are found in functions of a/h^*, R_n, c_1 and T for the thick FGM plates. The natural frequencies ω_{1n} are oscillating and going to around 0.005258/s with values of n for a/h^*= 5 and R_n = 10. Also the ω_{1n} are oscillating and going to around 0.008937/s with values of n for a/h^*=10 and R_n = 10.

Declaration of conflicting interests

The author(s) declared no potential conflicts of interest with respect to the research, authorship, and/or publication of this article.

References

[1] Gunasekaran V, Pitchaimani J, Chinnapandi LBM (2020) Analytical investigation on free vibration frequencies of polymer nano composite plate: effect of graphene grading and non-uniform edge loading. Materials Today Communications 24:100910.

[2] Vinyas M (2020) On frequency response of porous functionally graded magneto-electro-elastic circular and annular plates with different electro-magnetic conditions using HSDT. Composite Structures 240:112044.

[3] Alaimo A, Orlando C, Valvano S (2019) Analytical frequency response solution for composite plates embedding viscoelastic layers. Aerospace Science and Technology 92:429–445.

[4] Vinyas M, Sunny KK, Harursampath D, Nguyen-Thoi T, Loja MAR (2019) Influence of interphase on the multi-physics coupled frequency of three-phase smart magneto-electro-elastic composite plates. Composite Structures 226:111254.

[5] Karsh PK, Mukhopadhyay T, Chakraborty S, Naskarf S, Dey S (2019) A hybrid stochastic sensitivity analysis for low-frequency vibration and low-velocity impact of functionally graded plates. Composites Part B: Engineering 176:107221.

[6] Gao P, Climente A, Sánchez-Dehesa J, Wu L (2019) Single-phase metamaterial plates for broadband vibration suppression at low frequencies. Journal of Sound and Vibration 444:108–126.

[7] Geng J, Zhang X, Chen X, Wang C, Xiang J (2018) Mid-frequency dynamic characteristics prediction of thin plate based on B-spline wavelet on interval finite element method. Applied Mathematical Modelling 62:526–541.

[8] Morozov EV, Lopatin AV (2018) Fundamental frequency of fully clamped antisymmetric angle-ply laminated plates with structural anisotropy. Composite Structures 202:530–538.

[9] Lee MK, Fouladi MH, Namasivayam SN (2017) Natural frequencies of thin rectangular plates using homotopy-perturbation method. Applied Mathematical Modelling 50:524–543.

[10] Rezaei AS, Saidi AR, Abrishamdari M, Pour Mohammadi MH (2017) Natural frequencies of functionally graded plates with porosities via a simple four variable plate theory: an analytical approach. Thin-Walled Structures 120:366–377.

[11] Hong CC (2020) Free vibration frequency of thick FGM spherical shells with simply homogeneous equation by using TSDT. Journal of the Brazilian Society of Mechanical Sciences and Engineering 42:159.

[12] Hong CC (2020) Free vibration frequency of thick FGM circular cylindrical shells with simply homogeneous equation by using TSDT. Advance in Technology Innovation 5:84–97.

[13] Hong CC (2014) Thermal vibration and transient response of magnetostrictive functionally graded material plates. European Journal of Mechanics A/Solids 43:78–88.

[14] Hong CC (2012) Rapid heating induced vibration of magnetostrictive functionally graded material plates. Transactions of the ASME, Journal of Vibration and Acoustics 134:021019.

[15] Hong CC (2013) Thermal vibration of magnetostrictive functionally graded material shells. European Journal of Mechanics A/Solids 40:114–122.

[16] Chi SH, Chung YL (2006) Mechanical behavior of functionally graded material plates under transverse load, part I: analysis. International Journal of Solids and Structures 43:3657–3674.

[17] Lee SJ, Reddy JN, Rostam-Abadi F (2004) Transient analysis of laminated composite plates with embedded smart-material layers. Finite Elements in Analysis and Design 40:463–483.

[18] Shen HS (2007) Nonlinear thermal bending response of FGM plates due to heat condition. Composites Part B: Engineering 38:201–215.

[19] Hong CC (2019) GDQ computation for thermal vibration of thick FGM plates by using fully homogeneous equation and TSDT. Thin-Walled Structures 135:78–88.

[20] Jha DK, Kant T, Singh RK (2013) Free vibration response of functionally graded thick plates with shear and normal deformations effects. Composite Structures 96:799–823.

[21] Kim YW (2005) Temperature dependent vibration analysis of functionally graded rectangular plates. Journal of Sound and Vibration 284:531–549.

[22] Duc ND, Lee J, Nguyen-Thoi T, Thang PT (2017) Static response and free vibration of functionally graded carbon nanotube-reinforced composite rectangular plates resting on Winkler–Pasternak elastic foundations. Aerospace Science and Technology 68:391–402.

[23] Ungbhakorn V, Wattanasakulpong N (2013) Thermo-elastic vibration analysis of third-order shear deformable functionally graded plates with distributed patch mass under thermal environment. Applied Acoustics 74:1045–1059.

[24] Hong CC (2021) Free vibration of thick FGM plates under TSDT and thermal environment. Proceedings of Engineering and Technology Innovation 17:21–31.

Appendix

The dynamic equilibrium differential equations can be presented in matrix form as follows [19]:

$$
\begin{bmatrix}
0 & 0 & 0 & 0 & 0 \\
0 & 0 & 0 & 0 & 0 \\
-c_1{}^2H_{11} & -4c_1{}^2H_{16} & -2c_1{}^2H_{12}-4c_1{}^2H_{66} & -4c_1{}^2H_{26} & -c_1{}^2H_{22} \\
0 & 0 & 0 & 0 & 0 \\
0 & 0 & 0 & 0 & 0
\end{bmatrix}
\times \left\{ \frac{\partial^4 w}{\partial x^4} \quad \frac{\partial^4 w}{\partial x^3 \partial y} \quad \frac{\partial^4 w}{\partial x^2 \partial y^2} \quad \frac{\partial^4 w}{\partial x \partial y^3} \quad \frac{\partial^4 w}{\partial y^4} \right\}^t
$$

$$
+\begin{bmatrix}
0 & 0 & 0 & 0 & 0 & 0 & 0 & 0 & -c_1E_{11} & -3c_1E_{16} & \begin{matrix}-c_1E_{12}\\-2c_1E_{66}\end{matrix} & -c_1E_{26} \\
0 & 0 & 0 & 0 & 0 & 0 & 0 & 0 & -c_1E_{16} & \begin{matrix}-c_1E_{12}\\-2c_1E_{66}\end{matrix} & -3c_1E_{26} & -c_1E_{22} \\
c_1E_{11} & 3c_1E_{16} & \begin{matrix}c_1E_{12}\\+2c_1E_{66}\end{matrix} & c_1E_{26} & c_1E_{16} & \begin{matrix}c_1E_{12}\\+2c_1E_{66}\end{matrix} & 3c_1E_{26} & c_1E_{22} & 0 & 0 & 0 & 0 \\
0 & 0 & 0 & 0 & 0 & 0 & 0 & 0 & \begin{matrix}-c_1F_{11}\\+c_1{}^2H_{11}\end{matrix} & \begin{matrix}-3c_1F_{16}\\+3c_1{}^2H_{16}\end{matrix} & \begin{matrix}-c_1F_{12}\\+c_1{}^2H_{12}\\-2c_1F_{66}\\+2c_1{}^2H_{66}\end{matrix} & \begin{matrix}-c_1F_{26}\\+c_1{}^2H_{26}\end{matrix} \\
0 & 0 & 0 & 0 & 0 & 0 & 0 & 0 & \begin{matrix}-c_1F_{16}\\+c_1{}^2H_{16}\end{matrix} & \begin{matrix}-2c_1F_{66}\\+2c_1{}^2H_{66}\\-c_1F_{12}\\+2c_1{}^2H_{12}\end{matrix} & \begin{matrix}-3c_1F_{26}\\+3c_1{}^2H_{26}\end{matrix} & \begin{matrix}-c_1F_{22}\\+c_1{}^2H_{22}\end{matrix}
\end{bmatrix}
$$

$$
\times \left\{ \frac{\partial^3 u^0}{\partial x^3} \quad \frac{\partial^3 u^0}{\partial x^2 \partial y} \quad \frac{\partial^3 u^0}{\partial x \partial y^2} \quad \frac{\partial^3 u^0}{\partial y^3} \quad \frac{\partial^3 v^0}{\partial x^3} \quad \frac{\partial^3 v^0}{\partial x^2 \partial y} \quad \frac{\partial^3 v^0}{\partial x \partial y^2} \quad \frac{\partial^3 v^0}{\partial y^3} \quad \frac{\partial^3 w}{\partial x^3} \quad \frac{\partial^3 w}{\partial x^2 \partial y} \quad \frac{\partial^3 w}{\partial x \partial y^2} \quad \frac{\partial^3 w}{\partial y^3} \right\}^t
$$

$$
+\begin{bmatrix}
0 & 0 & 0 & 0 & 0 & 0 & 0 & 0 \\
0 & 0 & 0 & 0 & 0 & 0 & 0 & 0 \\
\begin{matrix}c_1F_{11}\\-c_1{}^2H_{11}\end{matrix} & \begin{matrix}3c_1F_{16}\\-3c_1{}^2H_{16}\end{matrix} & \begin{matrix}2c_1F_{66}\\-2c_1{}^2H_{66}\\+c_1F_{12}\\-c_1{}^2H_{12}\end{matrix} & \begin{matrix}c_1F_{26}\\-c_1{}^2H_{26}\end{matrix} & \begin{matrix}c_1F_{16}\\-c_1{}^2H_{16}\end{matrix} & \begin{matrix}c_1F_{12}\\-c_1{}^2H_{12}\\+2c_1F_{66}\\-2c_1{}^2H_{66}\end{matrix} & \begin{matrix}3c_1F_{26}\\-3c_1{}^2H_{26}\end{matrix} & \begin{matrix}c_1F_{22}\\-c_1{}^2H_{22}\end{matrix} \\
0 & 0 & 0 & 0 & 0 & 0 & 0 & 0 \\
0 & 0 & 0 & 0 & 0 & 0 & 0 & 0
\end{bmatrix}
$$

$$
\times \left\{ \frac{\partial^3 \psi_x}{\partial x^3} \quad \frac{\partial^3 \psi_x}{\partial x^2 \partial y} \quad \frac{\partial^3 \psi_x}{\partial x \partial y^2} \quad \frac{\partial^3 \psi_x}{\partial y^3} \quad \frac{\partial^3 \psi_y}{\partial x^3} \quad \frac{\partial^3 \psi_y}{\partial x^2 \partial y} \quad \frac{\partial^3 \psi_y}{\partial x \partial y^2} \quad \frac{\partial^3 \psi_y}{\partial y^3} \right\}
$$

$$
+\begin{bmatrix}
A_{11} & 2A_{16} & A_{66} & A_{16} & A_{12}+A_{66} & A_{26} & 0 & 0 & 0 \\
A_{16} & A_{12}+A_{66} & A_{26} & A_{66} & 2A_{26} & A_{22} & 0 & 0 & 0 \\
0 & 0 & 0 & 0 & 0 & 0 & \begin{matrix} -3c_1(2D_{55} \\ -3c_1F_{55}) \\ +A_{55}+c_1{}^2 I_6 \dfrac{\partial^2}{\partial t^2} \end{matrix} & \begin{matrix} -6c_1(2D_{45} \\ -3c_1F_{45}) \\ +2A_{45} \end{matrix} & \begin{matrix} -3c_1(2D_{44} \\ -3c_1F_{44}) \\ +A_{44}+c_1{}^2 I_6 \dfrac{\partial^2}{\partial t^2} \end{matrix} \\
\begin{matrix} B_{11} \\ -c_1E_{11} \end{matrix} & \begin{matrix} 2B_{16} \\ -2c_1E_{16} \end{matrix} & \begin{matrix} B_{66} \\ -c_1E_{66} \end{matrix} & \begin{matrix} B_{16} \\ -c_1E_{16} \end{matrix} & \begin{matrix} B_{12}+B_{66} \\ -c_1E_{12} \\ -c_1E_{66} \end{matrix} & \begin{matrix} B_{26} \\ -c_1E_{26} \end{matrix} & 0 & 0 & 0 \\
\begin{matrix} B_{16} \\ -c_1E_{16} \end{matrix} & \begin{matrix} B_{12}+B_{66} \\ -c_1E_{12}-c_1E_{66} \end{matrix} & \begin{matrix} B_{26} \\ -c_1E_{26} \end{matrix} & \begin{matrix} B_{66} \\ -c_1E_{66} \end{matrix} & \begin{matrix} 2B_{26} \\ -2c_1E_{26} \end{matrix} & \begin{matrix} B_{22} \\ -c_1E_{22} \end{matrix} & 0 & 0 & 0
\end{bmatrix}
$$

$$
\times\left\{ \frac{\partial^2 u^0}{\partial x^2} \quad \frac{\partial^2 u^0}{\partial x \partial y} \quad \frac{\partial^2 u^0}{\partial y^2} \quad \frac{\partial^2 v^0}{\partial x^2} \quad \frac{\partial^2 v^0}{\partial x \partial y} \quad \frac{\partial^2 v^0}{\partial y^2} \quad \frac{\partial^2 w}{\partial x^2} \quad \frac{\partial^2 w}{\partial x \partial y} \quad \frac{\partial^2 w}{\partial y^2} \right\}^t
$$

$$
+\begin{bmatrix}
B_{11}-c_1E_{11} & 2B_{16}-2c_1E_{16} & B_{66}-c_1E_{66} & B_{16}-c_1E_{16} & \begin{matrix} B_{12}+B_{66} \\ -c_1E_{12}-c_1E_{66} \end{matrix} & B_{26}-c_1E_{26} \\
B_{16}-c_1E_{16} & \begin{matrix} B_{12}+B_{66} \\ -c_1E_{12}-c_1E_{66} \end{matrix} & B_{26}-c_1E_{26} & B_{66}-c_1E_{66} & 2B_{26}-2c_1E_{26} & B_{22}-c_1E_{22} \\
0 & 0 & 0 & 0 & 0 & 0 \\
\begin{matrix} D_{11}-2c_1F_{11} \\ +c_1{}^2H_{11} \end{matrix} & \begin{matrix} 2D_{16}-4c_1F_{16} \\ +2c_1{}^2H_{16} \end{matrix} & \begin{matrix} D_{66}-2c_1F_{66} \\ +c_1{}^2H_{66} \end{matrix} & \begin{matrix} D_{16}-2c_1F_{16} \\ +c_1{}^2H_{16} \end{matrix} & \begin{matrix} D_{12}+D_{66} \\ -2c_1F_{12}+c_1{}^2H_{12} \\ -2c_1F_{66}+c_1{}^2H_{66} \end{matrix} & \begin{matrix} D_{26}-2c_1F_{26} \\ +c_1{}^2H_{26} \end{matrix} \\
\begin{matrix} D_{16}-2c_1F_{16} \\ +c_1{}^2H_{16} \end{matrix} & \begin{matrix} D_{12}+D_{66} \\ -2c_1F_{12}+c_1{}^2H_{12} \\ -2c_1F_{66}+c_1{}^2H_{66} \end{matrix} & \begin{matrix} D_{26}-2c_1F_{26} \\ +c_1{}^2H_{26} \end{matrix} & \begin{matrix} D_{66}-2c_1F_{66} \\ +c_1{}^2H_{66} \end{matrix} & \begin{matrix} 2D_{26}-4c_1F_{26} \\ +2c_1{}^2H_{26} \end{matrix} & \begin{matrix} D_{22}-2c_1F_{22} \\ +c_1{}^2H_{22} \end{matrix}
\end{bmatrix}
$$

$$
\times\left\{ \frac{\partial^2 \psi_x}{\partial x^2} \quad \frac{\partial^2 \psi_x}{\partial x \partial y} \quad \frac{\partial^2 \psi_x}{\partial y^2} \quad \frac{\partial^2 \psi_y}{\partial x^2} \quad \frac{\partial^2 \psi_y}{\partial x \partial y} \quad \frac{\partial^2 \psi_y}{\partial y^2} \right\}^t
$$

$$
+\begin{bmatrix}
0 & 0 & c_1 I_3 \frac{\partial^2}{\partial t^2} & 0 & 0 & 0 & 0 & 0 \\
0 & 0 & 0 & c_1 I_3 \frac{\partial^2}{\partial t^2} & 0 & 0 & 0 & 0 \\
-c_1 I_3 \frac{\partial^2}{\partial t^2} & -c_1 I_3 \frac{\partial^2}{\partial t^2} & 0 & 0 & \begin{matrix} A_{55} - 6c_1 D_{55} \\ +9c_1^2 F_{55} \\ -c_1 J_4 \frac{\partial^2}{\partial t^2} \end{matrix} & \begin{matrix} A_{45} - 6c_1 D_{45} \\ +9c_1^2 F_{45} \end{matrix} & \begin{matrix} A_{45} - 6c_1 D_{45} \\ +9c_1^2 F_{45} \end{matrix} & \begin{matrix} A_{44} - 6c_1 D_{44} \\ +9c_1^2 F_{44} \\ -c_1 J_4 \frac{\partial^2}{\partial t^2} \end{matrix} \\
0 & 0 & \begin{matrix} 6c_1 D_{55} - 9c_1^2 F_{55} \\ -A_{55} + c_1 J_4 \frac{\partial^2}{\partial t^2} \end{matrix} & \begin{matrix} 6c_1 D_{45} - 9c_1^2 F_{45} \\ -A_{45} \end{matrix} & 0 & 0 & 0 & 0 \\
0 & 0 & \begin{matrix} 6c_1 D_{45} - 9c_1^2 F_{45} \\ -A_{45} \end{matrix} & \begin{matrix} 6c_1 D_{44} - 9c_1^2 F_{44} \\ -A_{44} + c_1 J_4 \frac{\partial^2}{\partial t^2} \end{matrix} & 0 & 0 & 0 & 0
\end{bmatrix}
$$

$$
\times \begin{Bmatrix} \frac{\partial u^0}{\partial x} & \frac{\partial v^0}{\partial y} & \frac{\partial w}{\partial x} & \frac{\partial w}{\partial y} & \frac{\partial \psi_x}{\partial x} & \frac{\partial \psi_x}{\partial y} & \frac{\partial \psi_y}{\partial x} & \frac{\partial \psi_y}{\partial y} \end{Bmatrix}^t
$$

$$
+\begin{bmatrix}
-I_0 \frac{\partial^2}{\partial t^2} & 0 & 0 & -J_1 \frac{\partial^2}{\partial t^2} & 0 \\
0 & -I_0 \frac{\partial^2}{\partial t^2} & 0 & 0 & -J_1 \frac{\partial^2}{\partial t^2} \\
0 & 0 & -I_0 \frac{\partial^2}{\partial t^2} & 0 & 0 \\
-J_1 \frac{\partial^2}{\partial t^2} & 0 & 0 & -A_{55} + 6c_1 D_{55} - 9c_1^2 F_{55} - K_2 \frac{\partial^2}{\partial t^2} & -A_{45} + 6c_1 D_{45} - 9c_1^2 F_{45} \\
0 & -J_1 \frac{\partial^2}{\partial t^2} & 0 & -A_{45} + 6c_1 D_{45} - 9c_1^2 F_{45} & -A_{44} + 6c_1 D_{44} - 9c_1^2 F_{44} - K_2 \frac{\partial^2}{\partial t^2}
\end{bmatrix}
\begin{Bmatrix} u^0 \\ v^0 \\ w \\ \psi_x \\ \psi_y \end{Bmatrix}
$$

$$
= \begin{Bmatrix} f_1 \\ f_2 \\ f_3 \\ f_4 \\ f_5 \end{Bmatrix} \tag{A1}
$$

where $I_i = \sum_{k=1}^{N^*} \int_k^{k+1} \rho^{(k)} z^i dz$, ($i$ = 0,1,2,…,6), in which N^* is total number of constituent layers,$\rho^{(k)}$ is the density of superscript k^{th} constituent ply. $J_i = I_i - c_1 I_{i+2}$, (i =1,4), $K_2 = I_2 - 2c_1 I_4 + c_1^2 I_6$ and the $f_1,\ldots, f_5$ are the derivative expression terms in thermal loads and mechanical loads.

The fully homogeneous equation can be presented in matrix form as follows [19]:

$$\begin{bmatrix} FH_{11}-\frac{I_0\lambda_{mn}}{I_0} & FH_{12} & FH_{13}+\frac{c_1I_3\left(\frac{m\pi}{a}\right)\lambda_{mn}}{I_0} & FH_{14}-\frac{J_1\lambda_{mn}}{I_0} & FH_{15} \\ FH_{12} & FH_{22}-\frac{I_0\lambda_{mn}}{I_0} & FH_{23}+\frac{c_1I_3\left(\frac{n\pi}{b}\right)\lambda_{mn}}{I_0} & FH_{24} & FH_{25}-\frac{J_1\lambda_{mn}}{I_0} \\ FH_{13}+\frac{c_1I_3\left(\frac{m\pi}{a}\right)\lambda_{mn}}{I_0} & FH_{23}+\frac{c_1I_3\left(\frac{n\pi}{b}\right)\lambda_{mn}}{I_0} & FH_{33}-[I_0+{c_1}^2I_6\left(\frac{m\pi}{a}\right)^2+{c_1}^2I_6\left(\frac{n\pi}{b}\right)^2]\lambda_{mn}/I_0 & FH_{34}+\frac{c_1J_4\left(\frac{m\pi}{a}\right)\lambda_{mn}}{I_0} & FH_{35}+\frac{c_1J_4\left(\frac{n\pi}{b}\right)\lambda_{mn}}{I_0} \\ FH_{14}-\frac{J_1\lambda_{mn}}{I_0} & FH_{24} & FH_{34}+\frac{c_1J_4\left(\frac{m\pi}{a}\right)\lambda_{mn}}{I_0} & FH_{44}-\frac{K_2\lambda_{mn}}{I_0} & FH_{45} \\ FH_{15} & FH_{25}-\frac{J_1\lambda_{mn}}{I_0} & FH_{35}+\frac{c_1J_4\left(\frac{n\pi}{b}\right)\lambda_{mn}}{I_0} & FH_{45} & FH_{55}-\frac{K_2\lambda_{mn}}{I_0} \end{bmatrix} \begin{Bmatrix} a_{mn} \\ b_{mn} \\ c_{mn} \\ d_{mn} \\ e_{mn} \end{Bmatrix} = \begin{Bmatrix} 0 \\ 0 \\ 0 \\ 0 \\ 0 \end{Bmatrix} \tag{A2}$$

where

$\lambda_{mn} = I_0{\omega_{mn}}^2$,

$FH_{11} = A_{11}(m\pi/a)^2 + A_{66}(n\pi/b)^2$,

$FH_{12} = (A_{12} + A_{66})(m\pi/a)(n\pi/b)$,

$FH_{13} = -c_1E_{11}(m\pi/a)^3 - (c_1E_{12} + 2c_1E_{66})(m\pi/a)(n\pi/b)^2$,

$FH_{14} = (B_{11} - c_1E_{11})(m\pi/a)^2 + (B_{66} - c_1E_{66})(n\pi/b)^2$,

$FH_{15} = (B_{12} + B_{66} - c_1E_{12} - c_1E_{66})(m\pi/a)(n\pi/b)$,

$FH_{22} = A_{66}(m\pi/a)^2 + A_{22}(n\pi/b)^2$,

$FH_{23} = -(c_1E_{12} + 2c_1E_{66})(m\pi/a)^2(n\pi/b) - c_1E_{22}(n\pi/b)^3$,

$FH_{24} = (B_{12} + B_{66} - c_1E_{12} - c_1E_{66})(m\pi/a)(n\pi/b)$,

$FH_{25} = (B_{66} - c_1E_{66})(m\pi/a)^2 + (B_{22} - c_1E_{22})(n\pi/b)^2$,

$$FH_{33} = A_{55}(m\pi/a)^2 + A_{44}(n\pi/b)^2 + c_1^2H_{11}(m\pi/a)^4 + (2c_1^2H_{12} + 4c_1^2H_{66})(m\pi/a)^2(n\pi/b)^2 \\ + c_1^2H_{22}(n\pi/b)^4 - 3c_1(2D_{55} - 3c_1F_{55})(m\pi/a)^2 - 3c_1(2D_{44} - 3c_1F_{44})(n\pi/b)^2,$$

$$FH_{34} = A_{55}m\pi/a - (c_1F_{11} - c_1^2H_{11})(m\pi/a)^3 - (2c_1F_{66} - 2c_1^2H_{66} + c_1F_{12} - c_1^2H_{12})(m\pi/a)(n\pi/b)^2 \\ -(6c_1D_{55} - 9c_1^2F_{55})(m\pi/a),$$

$$FH_{35} = A_{44}n\pi/b - (c_1F_{22} - c_1^2H_{222})(n\pi/b^3) - (2c_1F_{66} - 2c_1^2H_{66} + c_1F_{12} - c_1^2H_{12})(m\pi/a)^2(n\pi/b) \\ -(6c_1D_{44} - 9c_1^2F_{44})(n\pi/b),$$

$FH_{44} = (D_{11} - 2c_1F_{11} + c_1^2H_{11})(m\pi/a)^2 + (D_{66} - 2c_1F_{66} + c_1^2H_{66})(n\pi/b)^2 + A_{55} - 6c_1D_{55} + 9c_1^2F_{55}$,

$FH_{45} = (D_{12} + D_{66} - 2c_1F_{12} + c_1^2H_{12} - 2c_1F_{66} + c_1^2H_{66})(m\pi/a)(n\pi/b)$,

$$FH_{55} = (D_{66} - 2c_1F_{66} + c_1^2H_{66})(m\pi/a)^2 + (D_{22} - 2c_1F_{22} + c_1^2H_{22})(n\pi/b)^2 + A_{44} - 6c_1D_{44} + 9c_1^2F_{44},$$

$$A_{11} = \frac{h^*}{1-\left(\frac{\nu_1+\nu_2}{2}\right)^2}\left(\frac{R_nE_1+E_2}{R_n+1}\right),$$

$$E_{11} = \frac{(h^*)^4(E_2-E_1)}{1-\left(\frac{\nu_1+\nu_2}{2}\right)^2}\left[\frac{1}{R_n+4} - \frac{3}{2(R_n+3)} + \frac{3}{4(R_n+2)} - \frac{1}{8(R_n+1)}\right],$$

$$F_{11} = \frac{(h^*)^5}{1-\left(\frac{\nu_1+\nu_2}{2}\right)^2}\left\{(E_2-E_1)\left[\frac{1}{R_n+5} - \frac{2}{R_n+4} + \frac{1}{R_n+3} - \frac{1}{2(R_n+2)} + \frac{1}{16(R_n+1)}\right] + \frac{E_1}{80}\right\},$$

$$H_{11} = \frac{(h^*)^7}{1-\left(\frac{\nu_1+\nu_2}{2}\right)^2}\left\{(E_2-E_1)\left[\frac{1}{R_n+7} - \frac{3}{R_n+6} + \frac{13}{4(R_n+5)} - \frac{2}{R_n+4} + \frac{13}{16(R_n+3)}\right.\right.$$
$$\left.\left. - \frac{3}{16(R_n+2)} + \frac{1}{64(R_n+1)}\right] + \frac{E_1}{448}\right\},$$

$$H_{44} = \frac{k_\alpha(h^*)^6(E_2-E_1)}{2\left(1+\frac{\nu_1+\nu_2}{2}\right)}\left[\frac{1}{R_n+6} - \frac{5}{2(R_n+5)} + \frac{2}{R_n+4} - \frac{1}{R_n+3} + \frac{5}{64(R_n+2)} - \frac{1}{32(R_n+1)}\right]$$

where E_1 and E_2 are the Young's modulus, ν_1 and ν_2 are the Poisson's ratios of the thick FGM constituent material 1 and material 2, respectively.

Assuming that $I_1 = I_3 = J_1 = 0$, $B_{ij} = E_{ij} = 0$, $A_{16} = A_{26} = 0$, $D_{16} = D_{26} = 0$ and $A_{45} = D_{45} = F_{45} = 0$ in the (A2), the simply homogeneous equation can be presented in matrix form as follows [24]:

$$\begin{bmatrix} FH_{11}-\lambda_{mn} & FH_{12} & 0 & 0 & 0 \\ FH_{12} & FH_{22}-\lambda_{mn} & 0 & 0 & 0 \\ 0 & 0 & FH_{33}-\lambda_{mn} & FH_{34} & FH_{35} \\ 0 & 0 & FH_{34} & FH_{44}-\frac{K_2}{I_0}\lambda_{mn} & FH_{45} \\ 0 & 0 & FH_{35} & FH_{45} & FH_{55}-\frac{K_2}{I_0}\lambda_{mn} \end{bmatrix} \begin{Bmatrix} a_{mn} \\ b_{mn} \\ c_{mn} \\ d_{mn} \\ e_{mn} \end{Bmatrix} = \begin{Bmatrix} 0 \\ 0 \\ 0 \\ 0 \\ 0 \end{Bmatrix} \tag{A3}$$